Spatially linked asperities of the 2006–2007 great Kuril earthquakes revealed by GPS

Grigory M. Steblov,[1,2] Mikhail G. Kogan,[2] Boris V. Levin,[3] Nikolai F. Vasilenko,[3] Alexander S. Prytkov,[3] and Dmitry I. Frolov[4]

Received 3 August 2008; revised 14 October 2008; accepted 17 October 2008; published 27 November 2008.

[1] In 2006–2007, two great earthquakes ruptured the center of the Kuril subduction zone: first, the interplate thrust event, then the intraplate extensional event on the outer rise. The affected region was a seismic gap since 1915. Published patterns of slip differ for various seismic and tsunami inversions. The surface offsets that we measured with GPS on the Kuril Islands are sensitive to the total slip, including slow components beyond the seismic and tsunami band. We invert coseismic offsets and show that the asperities, or regions of high slip, are spatially linked for both earthquakes; this pattern suggests (although does not prove) that the first event triggered the second. For the 2006 earthquake, the asperity is very shallow, probably because of the absence of an accretionary prism. For the 2007 earthquake, our modeling suggests that the rupture occurred in the bent Pacific lithosphere to a depth of ~50 km. **Citation:** Steblov, G. M., M. G. Kogan, B. V. Levin, N. F. Vasilenko, A. S. Prytkov, and D. I. Frolov (2008), Spatially linked asperities of the 2006–2007 great Kuril earthquakes revealed by GPS, *Geophys. Res. Lett.*, *35*, L22306, doi:10.1029/2008GL035572.

1. Introduction

[2] In 2006, we installed a GPS array over the whole Kuril subduction zone several months before two great earthquakes with magnitudes >8 struck in the center of the zone (Figure 1). On 15 November 2006, a thrust event ruptured the subduction interface between the Pacific and North American plates; then on 13 January 2007, an extensional event ruptured the outer rise of the Pacific lithosphere near the Kuril trench. Hereafter these events are called the 2006 and 2007 earthquakes. The earthquakes struck at a distance of ~100 km from each other in the Kuril arc segment where such large events had not happened since 1915 [*Fedotov*, 1965] (http://earthquake.usgs.gov). The tsunami runup of the 2006 earthquake reached 20 m on the Kuril Islands [*Bourgeois et al.*, 2007].

[3] Various seismic, geodetic, and tsunami observations provide evidence that slip is nonuniform over the earthquake fault [*Konca et al.*, 2007; *Pritchard et al.*, 2007; *Ammon et al.*, 2008; *Fujii and Satake*, 2008]. It is generally recognized that the maximum slip occurs within fault regions called asperities, patches that repeatedly break in earthquakes [*Kanamori and Stewart*, 1978; *Lay et al.*, 1989; *Bürgmann et al.*, 2005; *Cross and Freymueller*, 2007]. Inversions of seismic and tsunami data resolve the rapid slip that occurs at seismic and tsunami periods, respectively [*Ammon et al.*, 2008; *Fujii and Satake*, 2008]. By contrast, the offsets measured with GPS are sensitive to the total slip comprising both rapid and slow components. Here we evaluate and analyze slip distributions and asperities of the 2006–2007 great Kuril earthquakes determined from coseismic offsets on the Kuril GPS Array.

2. GPS Data and Coseismic Offsets

[4] The GPS network used in this study includes five continuous (CGPS) and three survey-mode (SGPS) stations on the Kuril islands, and CGPS stations on Sakhalin Island and on Kamchatka Peninsula (Figure 1 and Tables S1 and S2 of the auxiliary material).[1] We processed GPS observations aggregated as daily sessions with the GAMIT/GLOBK software [*Herring et al.*, 2006]. Modeling of coseismic offsets from daily positions of CGPS stations is documented in Text S1. On days of earthquakes, we also estimated station positions every 30 s by kinematic GPS module TRACK included in GAMIT. From the kinematic solution on 15 November 2006, we infer that most of the GPS offset (>90%) occurred within 5 min and that estimates of offset based on daily and on 30-s solutions agree (Figure 2). A similar conclusion applies to the 2007 event, although with less certainty because of smaller offsets. To estimate coseismic offsets of SGPS stations, we removed their postseismic motion; for that purpose, we determined this motion from observations at CGPS stations (Text S1).

[5] The Kuril GPS Array allowed us to detect coseismic and postseismic surface offsets ranging from several millimeters to over half a meter in response to slip from each of the 2006–2007 earthquakes (Figure 3).

3. Method of Inversion and Constraints

[6] We used the constrained damped least squares [*Gill et al.*, 1984] to invert the observed coseismic offsets for slip distribution over a grid of the fault model (Figure 4a). The inversion minimizes the objective function

$$OBJ = \chi_r^2 + \lambda \sum_{j=1}^{M} m_j^2, \qquad (1)$$

[1]Institute of Physics of the Earth, Russian Academy of Sciences, Moscow, Russia.
[2]Lamont-Doherty Earth Observatory, Columbia University, Palisades, New York, USA.
[3]Institute of Marine Geology and Geophysics, Far Eastern Branch, Russian Academy of Sciences, Yuzhno-Sakhalinsk, Russia.
[4]Ioffe Physico-Technical Institute, Russian Academy of Sciences, St. Petersburg, Russia.

0094-8276/08/2008GL035572$05.00

[1]Auxiliary materials are available in the HTML. doi:10.1029/2008GL035572.

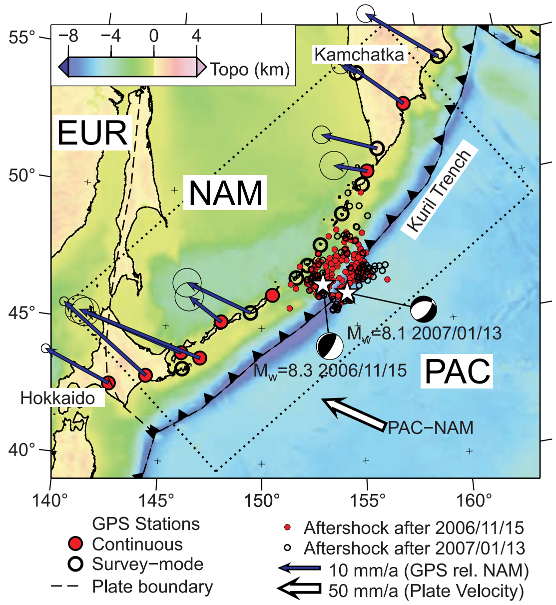

Figure 1. Tectonic sketch of the Kuril subduction zone and the Kuril GPS Array. Abbreviations for tectonic plates are NAM, EUR, and PAC, for the North American, Eurasian, and Pacific plates, respectively. Interseismic GPS velocities and their 1σ error ellipses are shown for those stations near the trench, which were observed long enough. Interseismic velocities are estimated relative to NAM; they reflect strain accumulation due to subduction. Vector PAC-NAM (a white arrow) shows the velocity of PAC relative to NAM. Epicenters (white stars) of the 2006–2007 earthquakes in this and subsequent figures were relocated by E.R. Engdahl. Focal mechanisms are from GCMT. Locations of aftershocks are from NEIC. The dotted rectangle denotes the region shown in Figure 3.

where $\chi_r^2 = \frac{1}{N}\sum_{i=1}^{N}\frac{1}{\sigma_i^2}\left(d_i - \sum_{j=1}^{M} G_{ij}m_j\right)^2$, d_i are the data; m_j are the model parameters; G_{ij} is the operator predicting the data from the model; N is the number of d_i; M is the number of m_j; σ_i is the RMS of d_i; λ is the positive damping factor. With larger λ, we get more stable solution with smaller variations in slip at the expense of increased data misfit χ_r^2. Conventionally, χ_r^2 is called the reduced chi-square of the inverse problem with the zeroth order regularization [*Press et al.*, 1994]. We used the method of F. Pollitz [*Pollitz*, 1996] to evaluate G_{ij} with the spherical layered Earth model PREM by summation of spherical harmonics 1–5000. The neglect of layering in the earth (as by *Takahashi and Kasahara* [2007]) would result in G_{ij} erroneous by about 50%.

[7] For each solution, we calculated the geodetic earthquake moment as $M_0^{GPS} = \sum_{i=1}^{L} \mu_i m_i S_i$, where μ_i, m_i, and S_i are the shear modulus, slip and area of the i-th grid cell, respectively; L is the number of cells. We constrain the search space by forcing the solutions to have the moment M_0^{GPS} in the range $0.5 \le M_0^{GPS}/M_0^{GCMT} \le 1.5$, where M_0^{GCMT} is the seismological moment from GCMT (http://www.globalcmt.org). The assumption of 50% uncertainty in M_0^{GCMT} appears reasonable in view of a wide range of moments for the Kuril 2006–2007 earthquakes estimated from teleseismic data (Table S3). We also constrain the variable rake of slip vectors over the grid: rake is allowed to depart within 20° from the best fitting uniform rake (Text S2). With these constraints imposed on the problem, we choose the damping factor λ in the inversion that results in $\chi_r^2 \approx 1$, that is, the data misfit is compatible with the data uncertainty.

[8] We set a value of μ = 40 GPa for the 2006 earthquake and a value of μ = 52 GPa for the 2007 earthquake as in [*Ammon et al.*, 2008]. There is no agreement among scientists on the value of μ best representing the strained subduction interface [*Bilek and Lay*, 1999; *Kreemer et al.*, 2006]. Our values of μ for both events agree to 10% with the values calculated from densities and seismic shear velocities of the global crustal model CRUST 2.0 [*Bassin et al.*, 2000].

4. Results

[9] We next characterize the results of our inversions of GPS offsets for the slip distributions.

[10] For the rupture of the 2006 event, we adopted the 150-km downdip width and the 230-km along-strike length (Figure 4a, fault planes AA′, BB′, and CC′); we were guided in this choice by distribution of the aftershocks that occurred between the 2006 and 2007 earthquakes (Figure S10a). The strike of the rupture was set to 221°, the orientation of the Kuril trench. We approximated the rupture on the subduction interface by three adjoining fault planes dipping 9°, 16°, and 22° to the northwest; the guidance for geometry of the interface was provided by depths and locations of shallow thrust earthquakes for the last three decades (Figure 4b and Text S2). Inversion was performed on a 3 × 4 grid constructed by dividing each of three rupture planes into four subfaults.

[11] The preferred coseismic slip model for the 2006 earthquake is N6A (Figure 4a) with the data misfit χ_r^2 = 1.0 in the feasible solution space (Figures 3a and S3). The maximum slip is 12 m on the southernmost subfault of the plane dipping 9° (Table S4a). To the west and north of the maximum, smaller slips of 10 and 6 m occur on neighboring subfaults dipping 16° and 9°. Model N6A has low slip (0–1 m) on the plane dipping 22°, which is the nearest plane to the island arc. To test the consistency among GPS offsets at various distances from the rupture, we repeated the inversion without the near-field stations KETO and MATU. The resulting slip model N6B (Figure S4) is quite similar to N6A; the offsets predicted by model N6B for excluded stations fit the data to 20%, a value compatible with RMS errors of measured coseismic offsets at these stations (Table S1). For both models N6A and N6B, the associated geodetic moment M_0^{GPS} reached the upper bound of the imposed constraint, i.e., M_0^{GPS} = 1.5 M_0^{GCMT}. Smaller M_0^{GPS} can be achieved by increasing the damping at the expense of larger data misfit. We attribute the substantial difference between M_0^{GPS} and M_0^{GCMT} to different geometries of the fault model: distributed slip on fault planes with variable dip in the geodetic inversion versus a point source on a single plane in GCMT.

[12] In inversions for slip of the 2007 earthquake, we set the length of the fault model to 230 km (Figure 4a, fault

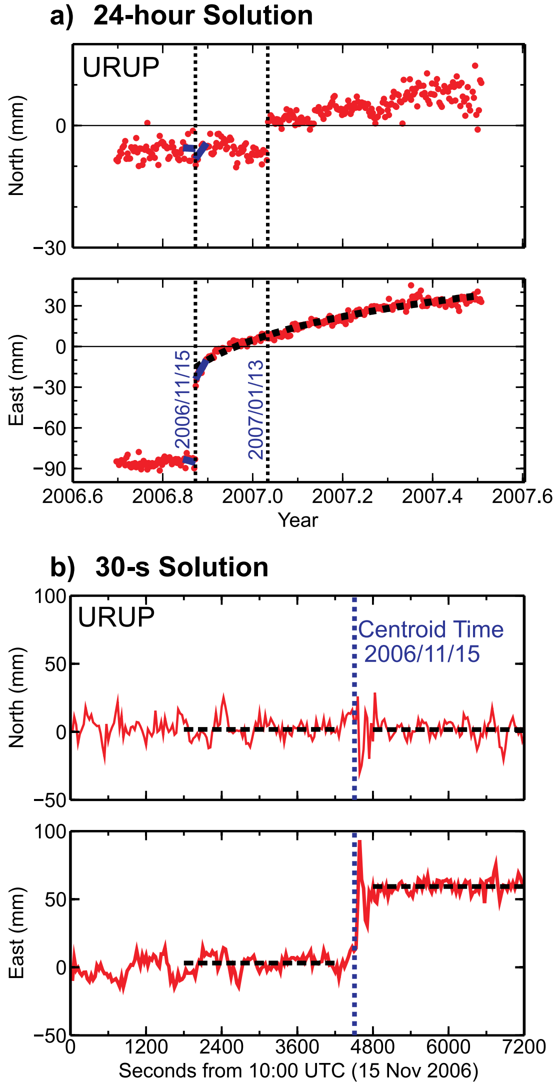

Figure 2. Time series of positions of the GPS station URUP. (a) The daily time series (red dots) for the period 2006.6–2007.6 relative to the North American plate. A dotted blue line is the logarithmic function best fitting postseismic afterslip. Short blue lines indicate first-order polynomial approximations of the daily time series over nine days before and nine days after the day of the earthquake. (b) The 30-s time series (red lines) before and after the centroid time of the 2006 earthquake, totally for two hours. Horizontal dashed lines indicate the average station position over 40 min before and after the centroid time.

plane DD′), the same as for the 2006 event and in agreement with spatial distribution of aftershocks (Figure S10a). For the 2007 earthquake, the downdip width is poorly constrained. Seismological inversions were performed with fault planes expanding to depths 30–50 km, but most of slip was found distributed at depths less than 25 km [*Ammon et al.*, 2008]. We constrained the model orientation (strike and dip) with the GCMT southeast dipping plane favored by the alignment of aftershocks. The strike was set to 41°, the reverse of the 2006 earthquake fault model and matching GCMT within 2°. A single rupture plane dipping 59° to the southeast was adopted from GCMT. At such steep dip, inversion of GPS offsets for slip is insensitive to large variations in the specified dip; for example, a variation by 10° changes the estimated slip by less than 1%. Inversion was carried out on a 1 × 4 grid constructed by dividing the single fault plane into four subfaults.

[13] Because of uncertainty in the fault width of the 2007 earthquake, we tested inversions with values of width 50 km (Figure 4a) and 25 km (Figure S5), resulting in slip models J7A and J7B, respectively. Model J7A exhibits the data misfit χ_r^2 = 0.7 (Figure 3b) and the geodetic moment M_0^{GPS} =1.5 M_0^{GCMT}. Stronger damping provides better agreement between geodetic and seismological moments (model J7C, Figure S6); with such damping, however, GPS offsets observed at several southern stations are significantly underpredicted. Slip distribution in model J7A peaks to 8 m at the southernmost subfault near the hypocenter and it decreases to 1 m at the northernmost subfault (Table S4b). Slip distribution in model J7B has the same pattern, but slips are about three times higher. We prefer model J7A

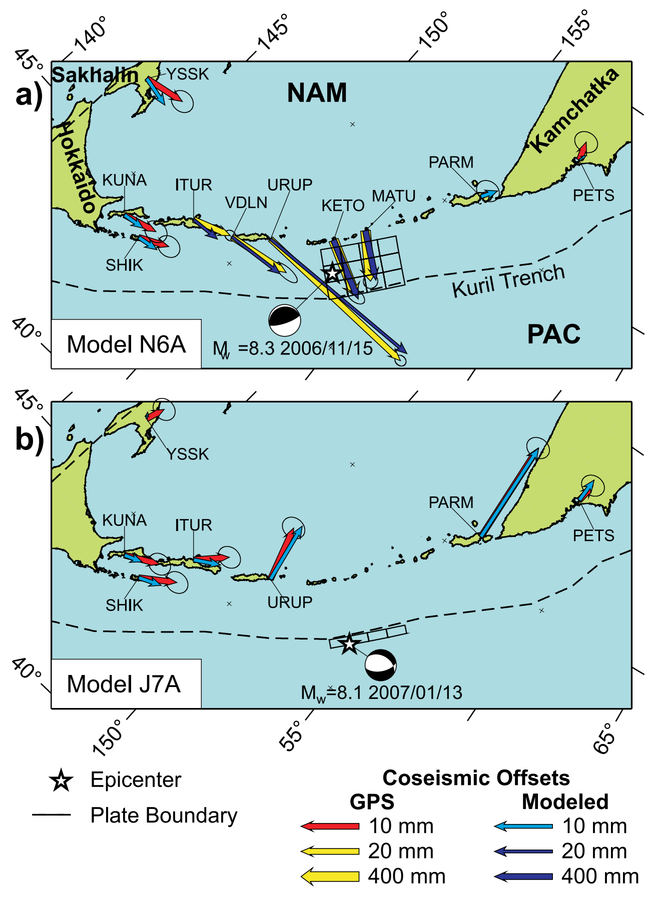

Figure 3. Observed and modeled coseismic offsets at GPS stations. Accuracy of observed offsets is indicated by 1σ error ellipses. Grids of the slip model subfaults are shown to compare with Figure 4a. (a) The 2006 earthquake, slip model N6A. The damping factor of the inversion $\lambda = 1.1 \times 10^{-3}$. The data misfit of inversion χ_r^2 = 1.00; geodetic moment $M_0 = 5.14 \times 10^{21}$ N·m. (b) The 2007 earthquake, slip model J7A. The damping factor of the inversion $\lambda = 1.4 \times 10^{-3}$. The data misfit of inversion χ_r^2 = 0.68; geodetic moment $M_0 = 2.66 \times 10^{21}$ N·m.

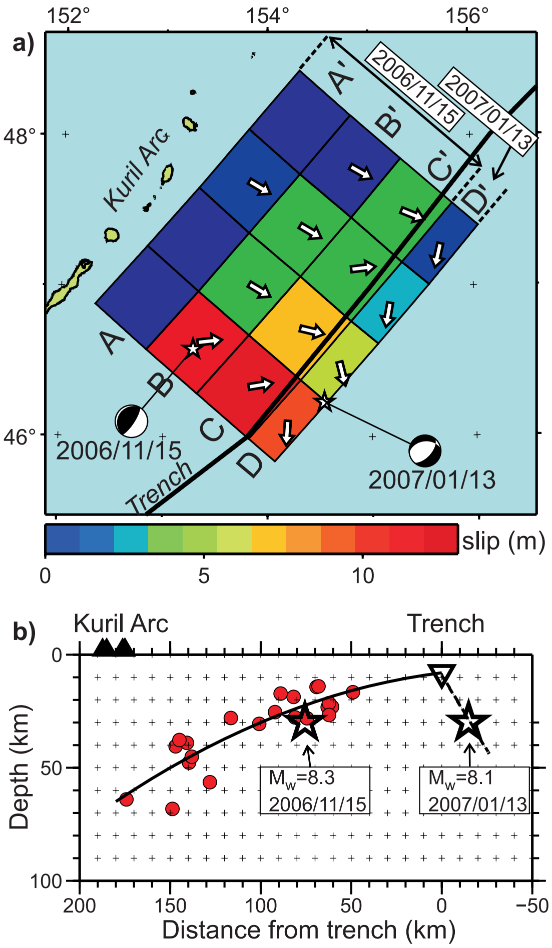

Figure 4. (a) Slip model N6A for the 2006 earthquake is estimated for fault planes AA′, BB′, and CC′ northwest-dipping 22°, 16°, and 9°, respectively. Slip model J7A for the 2007 earthquake is estimated for fault plane DD′ southeast-dipping 59°. Fault planes are shown as surface projections. Arrows indicate the motion of the hanging wall with respect to the footwall. Arrows are not shown for the grid cells that moved less than 0.01 m. (b) Cross section of shallow seismicity in the center of the Kuril subduction zone. Hypocenters of thrust events since 1976 (red circles) are projected from the region of the grid in Figure 4a. The solid curve is the 2nd-order polynomial best fitting the hypocenters. We assume it represents the subduction interface. The dashed line is the fault plane of the 2007 earthquake. The depth of its hypocenter is not well constrained. We tentatively set the depth to 30 km so that the hypocenter lies on the fault plane.

because the associated moment lies within the constraint imposed on the solution space.

[14] Our preferred slip models N6A and J7A for the 2006 and 2007 earthquakes, respectively, show nonuniform slip distributions. To test that this is not an artifact of the solution, we repeated inversions under the following constraint: the slip was prescribed to be uniform over each fault plane. The result of this exercise is significant, a factor of 2, increase in the data misfit χ_r^2 for both earthquakes, models N6C and J7D, respectively (Figures S7 and S8). For the 2006 earthquake, we also tested whether or not the high-slip patch on the shallowest, 9°-dipping fault plane is an artifact. For that purpose, we performed inversion allowing the slip only on the 16°-dipping fault plane (model N6D, Figure S9). However, this constraint results in a significant over-prediction of the offset at the near-field station KETO. We infer that nonuniform slip patterns are robust features of our preferred slip models.

5. Conclusions

[15] For the 2006 earthquake, the region of the highest slip outlines a shallow ruptured zone expanding from the trench bottom downward to a depth of only 22 km, i.e., lower edge of the model fault plane dipping 16°. The shallow rupture is also indicated by the location of the GCMT earthquake centroid near the trench. We attribute the shallow seismogenic fault in the central Kurils to the absence of the accretionary prism that controls the upper aseismic zone [*Marone and Scholz*, 1988; *Oleskevich et al.*, 1999; *Baba*, 2000]. By contrast, our modeling suggests that the 2007 earthquake ruptured the bent Pacific lithosphere to a depth of ~50 km, that is, to the neutral plane of stresses. Highest-slip patches, commonly known as asperities, from the 2006 and 2007 earthquakes are adjacent to each other; this correlation suggests (although does not prove) that the 2007 extensional event was triggered by redistribution of stresses following the 2006 thrust event.

[16] **Acknowledgments.** Kuril GPS observations between 2006 and 2008 were made possible in part by the Kuril Biocomplexity Project (NSF grant ARC-0508109; PI: B. Fitzhugh). J. Bourgeois generously helped to set up the GPS program on the Kurils. F.F. Pollitz provided his code for the deformation Green's function in the layered spherical Earth. E. R. Engdahl and G.L. Choy provided relocated positions of the Kuril earthquakes. This paper benefited from reviews by T.H. Dixon and an anonymous reviewer. UNAVCO Consortium added three GPS systems to our pool; J. Normandeau tested all GPS systems at UNAVCO. Figures were drawn with the GMT software [*Wessel and Smith*, 1998]. This study was funded in USA by NSF grants EAR-0715360 and EAR-0809718; in Russia by RFFI grants 080500197 and 070510070, and FEB RAS grants 06IICO08030 and 06IIIB08375. Lamont-Doherty Earth Observatory contribution 7216.

References

Ammon, C. J., H. Kanamori, and T. Lay (2008), A great earthquake doublet and seismic stress transfer cycle in the central Kuril Islands, *Nature*, *451*, 561–565.

Baba, K. (2000), A tectonic control on methane hydrate distribution at island arc system, *Eos Trans. AGU*, *83*(22), West. Pac. Meet. Suppl., Abstract S21A-02.

Bassin, C., G. Laske, and G. Masters (2000), The current limits of resolution for surface wave tomography in North America, *Eos Trans. American Geophysical Union*, *81*(48), Fall Meet. Suppl., Abstract S12A-03.

Bilek, S. L., and T. Lay (1999), Rigidity variations with depth along interplate megathrust faults in subduction zones, *Nature*, *400*, 443–446, doi:10.1038/22739.

Bourgeois, J., T. Pinegina, N. Razhegaeva, V. Kaistrenko, B. V. Levin, B. MacInnes, and E. Kravchunovskaya (2007), Tsunami runup in the middle Kuril Islands from the great earthquake of 15 Nov 2006, *Eos Trans. American Geophysical Union*, *88*(52), Fall. Meet. Suppl., Abstract S51C-02.

Bürgmann, R., M. G. Kogan, G. M. Steblov, G. Hilley, V. E. Levin, and E. Apel (2005), Interseismic coupling and asperity distribution along the Kamchatka subduction zone, *J. Geophys. Res.*, *110*, B07405, doi:10.1029/2005JB003648.

Cross, R. S., and J. T. Freymueller (2007), Plate coupling variation and block translation in the Andreanof segment of the Aleutian arc determined by subduction zone modeling using GPS data, *Geophys. Res. Lett.*, *34*, L06304, doi:10.1029/2006GL028970.

Fedotov, S. A. (1965), Regularities of distribution of large earthquakes of Kamchatka, Kuril Islands, and North-Eastern Japan, *Trans. Inst. Phys. Earth Acad. Sci. USSR*, *36*, 68–93.

Fujii, Y., and K. Satake (2008), Tsunami sources of the November 2006 and January 2007 great Kuril earthquakes, *Bull. Seismol. Soc. Am.*, *98*, 1559–1571, doi:10.1785/0120070221.

Gill, P. E., W. Murray, M. A. Saunders, and M. H. Wright (1984), Procedures for optimization problems with a mixture of bounds and general linear constraints, *ACM Trans. Math. Software*, *10*, 282–298.

Herring, T. A., R. W. King, and S. McClusky (2006), *Introduction to GAMIT/GLOBK*, release 10.3, 37 pp. Mass. Inst. of Tech., Cambridge.

Kanamori, H., and G. S. Stewart (1978), Seismological aspects of the Guatemala earthquake of February 4, 1976, *J. Geophys. Res.*, *83*, 3427–3434.

Konca, O., V. Hjorleifsdottir, T.-R. A. Song, J.-P. Avouac, D. Helmberger, C. Ji, K. Sie, R. Briggs, and A. Meltzner (2007), Rupture kinematics of the 2005 Mw 8.6 Nias-Simeulue earthquake from the joint inversion of seismic and geodetic data, *Bull. Seismol. Soc. Am.*, *97*, S307–S322, doi:10.1785/0120050632.

Kreemer, C., G. Blewitt, and F. Maerten (2006), Co- and postseismic deformation of the 28 March 2005 Nias Mw 8.7 earthquake from continuous GPS data, *Geophys. Res. Lett.*, *33*, L07307, doi:10.1029/2005GL025566.

Lay, T., L. Astiz, H. Kanamori, and D. H. Christensen (1989), Temporal variation of large intraplate earthquakes in coupled subduction zones, *Phys. Earth Planet. Inter.*, *54*, 258–312.

Marone, C., and C. H. Scholz (1988), The depth of seismic faulting and the upper transition from stable to unstable slip regimes, *Geophys. Res. Lett.*, *15*, 621–624.

Oleskevich, D. A., R. D. Hyndman, and K. Wang (1999), The updip and downdip limits to great subduction earthquakes: Thermal and structural models of Cascadia, south Alaska, SW Japan, and Chile, *J. Geophys. Res.*, *104*, 14,965–14,991.

Pollitz, F. (1996), Coseismic deformation from earthquake faulting on a layered spherical Earth, *Geophys. J. Int.*, *125*, 1–14.

Press, W. H., S. A. Teukolsky, W. T. Vetterling, and B. P. Flannery (1994), *Numerical Recipes in FORTRAN*, 2nd ed., 963 pp. Cambridge Univ. Press, Cambridge, U. K.

Pritchard, M. E., E. O. Norabuena, C. Ji, R. Boroschek, D. Comte, M. Simons, T. H. Dixon, and P. A. Rosen (2007), Geodetic, teleseismic, and strong motion constraints on slip from recent southern Peru subduction zone earthquakes, *J. Geophys. Res.*, *112*, B03307, doi:10.1029/2006JB004294.

Takahashi, H., and M. Kasahara (2007), Geodetic constraint on the slip distribution of the 2006 central Kuril earthquake, *Earth Planets Space*, *59*, 1095–1098.

Wessel, P., and W. H. F. Smith (1998), New, improved version of generic mapping tools released, *Eos Trans. AGU*, *79*, 579.

D. I. Frolov, Ioffe Physico-Technical Institute, Russian Academy of Sciences, 26 Politekhnicheskaya Street, St. Petersburg 194021, Russia.

M. G. Kogan, Lamont-Doherty Earth Observatory, Columbia University, 61 Route 9W, Palisades, NY 10964, USA. (kogan@ldeo.columbia.edu)

G. M. Steblov, Institute of Physics of the Earth, Russian Academy of Sciences, 10 B. Gruzinskaya Street, Moscow 123995, Russia. (steblov@gps.gsras.ru)

B. V. Levin, A. S. Prytkov, and N. F. Vasilenko, Institute of Marine Geology and Geophysics, Far Eastern Branch, Russian Academy of Sciences, 5 Nauka Street, Yuzhno-Sakhalinsk 693022, Russia.